

shown in Fig. 2. The breadth of the transition (i.e., when the shielding between the two coils by the superconducting foil is at least 90% complete) is indicated by the length of the vertical lines. On each side of the single-phase bcc region there is an abrupt change in the transition temperature. The highest transition temperature (4.12°K) occurs at 60 at.% Ti, where normally the equilibrium structure is fcc with $T_c = 2.50^\circ\text{K}$. This transition temperature of 4.12°K is higher than any of the equilibrium alloys which occur across the phase diagram, including pure indium.

Several interesting points can be observed from the present study. (1) With the present rate of quenching estimated at the order of several million degrees per second,⁹ the bcc to hcp transformation of pure Tl could not be suppressed. This is indicative of the diffusionless nature of the transformation. When In is added, this

⁹ P. Predecki, A. W. Mullendore, and N. J. Grant, *Trans. AIME* **233**, 1581 (1965).

transformation is gradually retarded, but the full retention of the bcc structure is achieved only when the In concentration reaches the eutectoidal composition of ~ 17 at.%. The abrupt change in T_c near 83 at.% Tl is definitely associated with the presence of the hcp phase. (2) The fact that the presence of the hcp phase lowers the T_c 's certainly indicates that the bcc form of Tl would have higher T_c than the hcp form if the former could be retained. By linearly extrapolating the T_c versus composition curve to zero In content, the T_c of bcc Tl is estimated to be $3.0 \pm 0.1^\circ\text{K}$ (Fig. 2). (3) Undoubtedly the bcc-fcc transformation induces a 1.2°K difference in T_c . Thus, in the In-Tl system, the bcc phase has the highest T_c among the three most common crystal structures occurred in metals (e.g., bcc, fcc, and hcp). However, the T_c 's of the fcc and hcp phases can not be compared directly.

The authors are indebted to Professor P. Duwez for his encouragement and to John McCoy for assistance in experiments.

Magnetic Properties of Some Rare-Earth Alloys at High Pressures

D. B. McWHAN AND A. L. STEVENS

Bell Telephone Laboratories, Murray Hill, New Jersey

(Received 22 August 1966)

The Néel and Curie temperatures of some alloys of the heavy rare-earth metals with each other and with yttrium have been measured as functions of pressure up to ~ 85 kbar. The initial slopes (dT/dP) are approximately proportional to the average de Gennes function ($\sum_i c_i (g_i - 1)^2 J_i (J_i + 1)$). In the molecular field approximation with a first-order correction for the anisotropy energy, the change in the exchange interaction with lattice parameter is given by $k^{-1} dJ(\mathbf{Q})/da = (42 \pm 6)^\circ\text{K}/\text{\AA}$. It is suggested that this is caused mainly by a change in the generalized conduction-electron susceptibility with pressure. A polymorphic transition from a hexagonal-close-packed structure to a Sm-type structure is found with increasing pressure in many of these alloys, and the Sm-type phase has two ordering temperatures. The higher ordering temperature of the Sm-type phase is 10% lower than that of the hcp phase, and the two ordering temperatures in the Sm-type phase differ by 17%.

IN the pressure range from 1 bar to 100 kbar, both volume changes of $\sim 15\%$ and polymorphic transitions occur in the heavy rare-earth metals. Their magnetic properties change appreciably under these conditions, and the present study completes a survey of the effect of pressure of the Néel and Curie temperatures above 77°K of rare-earth metals and of alloys of the heavy rare earths with each other and with Y. Previous papers include: (1) The elements Gd, Tb, Dy, and Ho,¹ (2) Eu and EuO,² and (3) a preliminary report on the Tb-Y alloys.³ In all of the metals and

alloys studied, the magnetic ordering temperatures decrease with increasing pressure and, therefore, the magnetic energies are positive functions of volume. The trend in crystal structures observed in the rare-earth metals with decreasing atomic number is also observed with increasing pressure,^{4,5} and many of the heavy rare-earth metals transform from the hexagonal close-packed structure (hcp) to the Sm-type structure with increasing pressure. In the latter structure the initial susceptibility suggests that two independent ordering temperatures exist and that ferromagnetism does not occur above 77°K .

¹ D. B. McWhan and A. L. Stevens, *Phys. Rev.* **139**, A682 (1965).

² D. B. McWhan, P. C. Souers, and G. Jura, *Phys. Rev.* **143**, 385 (1966).

³ D. B. McWhan, E. Corenzwit, and A. L. Stevens, *J. Appl. Phys.* **37**, 1355 (1966).

⁴ A. Jayaraman and R. C. Sherwood, *Phys. Rev. Letters* **12**, 22 (1964).

⁵ A. Jayaraman and R. C. Sherwood, *Phys. Rev.* **134**, A691 (1964).

TABLE I. Data for some rare-earth elements and alloys.

Sample	Characterization			Change in T_N with P			Phase transition		High-pressure phase $T_{N2a}-T_{N2b}$	
	Wt. Loss during prep. %	Lattice constants a/a_{Tb} ±0.0005 c/c_{Tb} ±0.0005		T_N (°K) 1 bar Literature ^a Extrap.	(dT_N/dP) °K/Kbar ±10%	P range kbar 5 to	$T_{N1}-T_{N2a}$ °K	At P kbar		
Tb	...	1.0000	1.0000	228	227	1.08	34	18	35	29
95% Tb-5% Y	0.24	1.0019	1.0015	...	219	0.80	30	17	30	28
90% Tb-10% Y	0.18	1.0025	1.0010	211	213	0.77	30	17	40	26
85% Tb-15% Y	0.19	1.0033	1.0007	...	207	0.70	47	17	52	26
80% Tb-20% Y	0.17	1.0042	1.0032	196	201	0.63	45	15	60	24
70% Tb-30% Y	0.06	1.0041	1.0037	183	186	0.52	45	15	87	21
60% Tb-40% Y	0.09	1.0073	1.0032	169	168	0.41	55
50% Tb-50% Y	0.07	1.0085	1.0035	149	149	0.32	53
40% Tb-60% Y	0.03	1.0087	1.0038	129	136	0.32	70
30% Tb-70% Y	0.02	1.0102	1.0043	111	111	0.28	85
Dy	179	182	0.62	40	13	49	25
67.5% Tb-32.5% Y	0.14	1.0052	1.0021	...	182	0.5	45	13	60	21
67.5% Tb-32.5% Lu	0.70	0.9878	0.9931	...	175	0.51	75
57% Tb-43% Er	0.84	0.9966	0.9919	...	181	0.6	75	15	85	21
45% Gd-55% Y	0.08	1.0123	1.0092	...	161	0.59	75	...	~85	...
45% Gd-55% Lu	0.91	0.9906	0.9917	...	147	0.5	45
34.3% Gd-65.7% Er	0.65	0.9961	0.9928	...	144	0.44	75	...	~85	...
	98	0.36	60
Gd	291.8 ^b	291	1.63	25	38	25	20
Ho	133	133	0.48	65	9	76	(15-20)

^a H. R. Child, W. C. Koehler, E. O. Wollan, and J. W. Cable. Phys. Rev. **138**, A1655 (1965).
^b M. Griffel, R. E. Skochoopole, and F. H. Spedding. Phys. Rev. **93**, 675 (1954).

It is known at 1 atm that the magnetic properties of these materials are smooth functions of the average de Gennes's function $\sum_i c_i (g_i - 1)^2 J_i (J_i + 1)$ where c_i is the atom fraction of the i th element.⁶ To complete the present study, two sets of experiments were performed. First, a series of mixed alloys having the same value of $\sum_i c_i (g_i - 1)^2 J_i (J_i + 1)$ were studied, and second, the effect of diluting Tb with the nonmagnetic element Y was investigated.

EXPERIMENTAL

The samples were prepared by arc melting. Appropriate mixtures of Gd, Tb, Er, Lu (Research Chemicals Inc., stated purity 99.9%) and Y (American Smelting and Refining Company—stated purity 99.9%) were melted several times to assure homogeneity. The weight lost during preparation is listed in Table I, and this is taken as a measure of the maximum deviation from the desired composition that could have resulted. Guinier x-ray powder patterns (internally calibrated with KCl) taken with Cu K_α radiation only showed reflections of the hcp structure, and the percent change in the lattice parameters from those of pure terbium are given in Table I.

The high-pressure apparatus has been described.¹ The pressure measurement is relative to the transitions in the electrical resistivity of bismuth at 25.4, 26.9, and 82 kbar, and the error in the absolute pressure is $\pm 5\%$. The temperature was measured relative to 77°K with

a Chromel-Alumel thermocouple. The quasi-hydrostatic pressure was transmitted to the sample by AgCl. The initial susceptibility was measured by a transformer method with a 6-kc signal producing a field of ~ 1 Oe at the sample. An improvement in the techniques described in Ref. 1 has been made by winding the transformer in a bifilar manner and by balancing the secondary signal to zero at $\sim 0^\circ\text{C}$ on cooling at each pressure with a variable resistance-inductance circuit. Therefore, the relative change with temperature of the initial susceptibility (χ_i) in arbitrary units is measured. The paramagnetic-to-antiferromagnetic transition (Néel) temperature T_N was taken as the cusp, and the antiferromagnetic-to-ferromagnetic transition (Curie) temperature T_c was taken as the inflection point in the sharp rise in χ_i that occurs at lower temperatures. (See Fig. 2.) The cusps seen in the high-pressure phases are denoted as $T_N(2a)$ and $T_N(2b)$. The error in the measurement of the transition temperature is $\sim \pm 2^\circ\text{K}$.

RESULTS

Because of our present, rather poor understanding of the effect of quasi-hydrostatic pressure on these systems, a rather extensive presentation of the detailed results is given. First, the alloy Tb_{0.95}Y_{0.05} is presented, as the other alloys show all or some of the same features. Second, the alloys with $\sum_i c_i (g_i - 1)^2 J_i (J_i + 1) = 7.08$ (Dy) are discussed, and finally the Tb_cY_{1-c} alloys are summarized.

A set of curves of χ_i versus T obtained on warming at

⁶ W. C. Koehler, J. Appl. Phys. **36**, 1078 (1965).

different pressures for $Tb_{0.95}Y_{0.05}$ are shown in Figs. 1 and 2. The Néel temperature shows little or no temperature hysteresis in the cooling and warming cycles. However, the Curie temperature shows a marked hysteresis ($\sim 9^\circ K$). The curves of χ_i obtained on cooling and warming exhibit a large difference in magnitude and in shape below the Curie temperature. The cooling curves at different pressures below 30 kbar are similar in shape, but the warming curves exhibit two broad maxima as shown in Fig. 2. A similar effect was observed in Tb and Gd. However in Gd the two maxima were observed both in the cooling and warming cycles. A typical curve for Gd at 20 kbar was given in Fig. 6 of Ref. 1.

At pressures above 30 kbar, χ_i drops over a factor of 10, and the sharp rise indicative of the transition from the antiferromagnetic to the ferromagnetic state disappears. As in the elements Gd, Tb, Dy, and Ho, two new peaks appear at lower temperatures. The pressure at which the peaks first appear and their amplitude depend quite strongly on the time the sample is held at a particular pressure and possibly on sample preparation. In different runs on the $Tb_{0.95}Y_{0.05}$ alloy, the two peaks first appeared over a range of pressure from 30 to 60 kbar. In the run shown in Fig. 1 the sample was held at high pressure for approximately a week, and the different holding times are shown in the figure.

The alloys with the average de Gennes's function, $\sum_i c_i (g_i - 1)^2 J_i (J_i + 1)$, equal to that of Dy (7.08) are

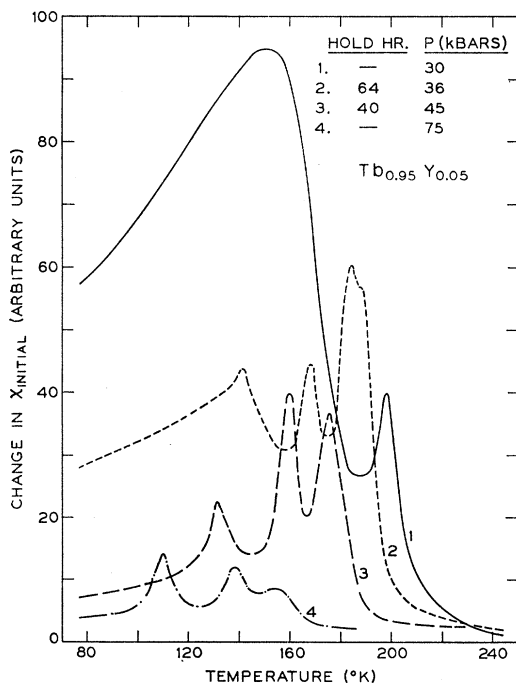


FIG. 1. Comparison of different isobars of the change in relative initial susceptibility versus temperature. The curve for $Tb_{0.95}Y_{0.05}$ at 30 kbar is reduced by a factor of 10. Holding times are the number of hours the sample was held at the appropriate pressure before obtaining the isobar. All curves are from one experiment.

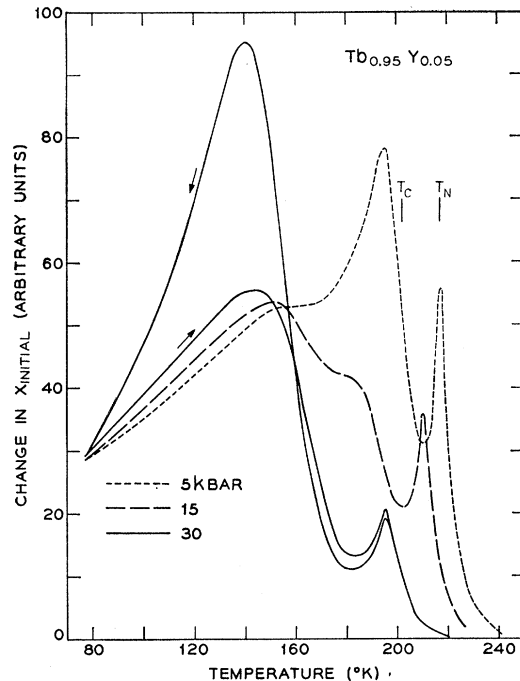


FIG. 2. Comparison of the cooling and warming curves at 30 kbar and the warming curves at 5, 15, and 30 kbar in $Tb_{0.95}Y_{0.05}$.

listed at the bottom of Table I. All of the measurements on each sample were carried out in the same sequence which was: isobar at 5 kbar; the Bi calibration points at 25.4 and 26.9 kbar at room temperature; isobars at 30 and 45 kbar; sample held at 45 kbar overnight; isobars at 60 and 75 kbar; Bi calibration at 82 kbar and room temperature; final isobar at 85 kbar. This sequence represents a compromise between maximum coverage of the available pressure range and average lifetime of each pressure experiment. The results from the two best runs on Dy (Ref. 1) and the three terbium alloys ($Tb_{0.675}Y_{0.325}$, $Tb_{0.675}Lu_{0.325}$, and $Tb_{0.57}Er_{0.43}$) are shown in Fig. 3. Qualitatively, all four materials show the same general features: namely similar slopes and the appearance of two new peaks at high pressures. The pressure at which the polymorphic transition occurs is a function of the alloy. The transition in Dy has been shown to occur at ~ 45 kbar. The transformation in $Tb_{0.675}Y_{0.325}$ occurs between 45 and 60 kbar but in $Tb_{0.675}Lu_{0.325}$, $Tb_{0.57}Er_{0.43}$, $Gd_{0.45}Y_{0.55}$, and $Gd_{0.343}Er_{0.657}$ it does not occur below 75 kbar. As all samples were prepared and run in the same way, this would appear to represent a real difference in the transition pressure.

A smooth curve of T_N versus P can not be drawn through all the data for the cusp corresponding to the ordering of the hcp phase. There is a discontinuity of approximately -7° when the two new peaks appear as the sluggish polymorphic transition begins to occur (see Fig. 3). The splitting of the first peak in the second curve of Fig. 1 may reflect this discontinuity as there

may have been regions across the sample where the polymorphic transition had and had not been initiated. This apparent lowering of the ordering temperature in the two-phase region explains a discrepancy in the initial slopes (dT/dP) noted in Ref. 1. Fitting all of our data for Gd and Dy by straight lines led to slopes of $-(1.72 \pm 0.07)^\circ\text{K}/\text{kbar}$ (Gd) and $-(0.66 \pm 0.04)^\circ\text{K}/\text{kbar}$ (Dy), and the magnitude of these slopes was slightly larger than had been reported in the literature. If only the data obtained below the polymorphic transition are used, the slopes are: $-(1.63 \pm 0.07)$ (Gd) and $-(0.62 \pm 0.04)^\circ\text{K}/\text{kbar}$ (Dy), and these are in better agreement with the literature. All the data obtained on the elements and alloys have been reinterpreted using only the data obtained at pressures below the polymorphic transition and the resulting slopes are listed in Table I.

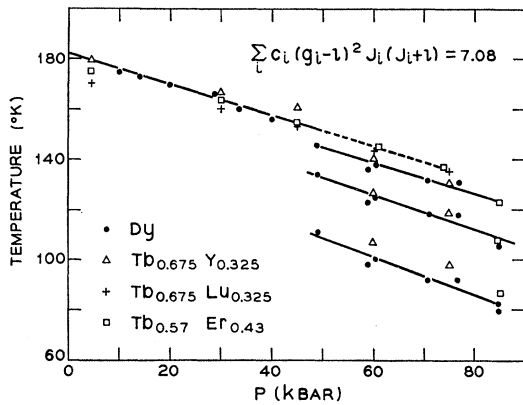


FIG. 3. Comparison of the effect of pressure on the ordering temperatures of different alloys with an average De Gennes' function equal to that of Dy.

The alloys containing Gd had lower Néel temperatures than the alloys with Tb, and the results are tabulated in Table I. The alloy $\text{Gd}_{0.343}\text{Er}_{0.657}$ was particularly interesting because it might have three ordering temperatures similar to pure Er. With decreasing temperature a structure with a sinusoidal variation of the c -axis component appears at 80°K in Er; a transition to a quasi-antiphase domain structure occurs at 52°K , and a transition to a conical ferromagnetic structure occurs at 20°K .⁷ Measurements of the magnetization of $\text{Gd}_{0.343}\text{Er}_{0.657}$ versus temperature made at 1 atm by Sherwood⁴ with a pendulum magnetometer confirmed the existence of three transitions in this alloy. (Bozorth and Gambino report only the upper two transition temperatures.)⁸ The susceptibility above 180°K follows a Curie-Weiss Law with an effective moment $\bar{\mu} = 8.87\mu_B$

⁷ J. W. Cable, E. O. Wollan, W. C. Koehler, and M. K. Wilkinson, *Phys. Rev.* **140**, A1896 (1965).

⁸ R. M. Bozorth and R. Gambino, in *Proceedings of the International Conference on Magnetism, Nottingham, 1964* (The Institute of Physics and The Physical Society, London, 1965), p. 263; Fifth Rare Earth Research Conference, Iowa State University, 1965 (unpublished).

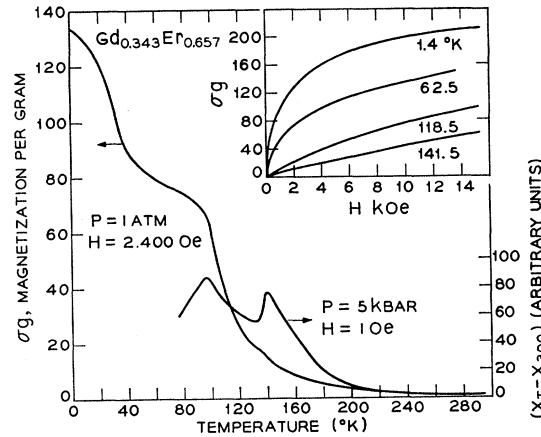


FIG. 4. Comparison of magnetization versus temperature at $P=1$ atm. and $H=2,400$ Oe with the change in relative initial susceptibility versus temperature at $P=5$ kbar and $H=1$ Oe for $\text{Gd}_{0.343}\text{Er}_{0.657}$. In the inset, magnetization versus field curves for each of the different magnetic regions are plotted.

and $\theta_p = 150^\circ\text{K}$. In Fig. 4 the magnetization measurements at $H=2,400$ Oe and $P=1$ atm are compared with the initial susceptibility measurements at $H \approx 1$ Oe and $P=5$ kbar. Assuming that the three transitions observed in $\text{Gd}_{0.343}\text{Er}_{0.657}$ are similar to the three in Er, the pressure dependence of the paramagnetic to sinusoidal transition is $-0.44^\circ\text{K}/\text{kbar}$, and the pressure dependence of the sinusoidal to antiphase domain transition is $-0.36^\circ\text{K}/\text{kbar}$.

The results for the $\text{Tb}_c\text{Y}_{1-c}$ system are shown in Figs. 5, 6, and 7, and summarized in Table I. In Fig. 5, the extrapolated T_N versus P curve for pure Tb from Ref. 1 forms an envelope for the other alloys. This is illustrated for $\text{Tb}_{0.45}\text{Y}_{0.05}$ where initially the Néel

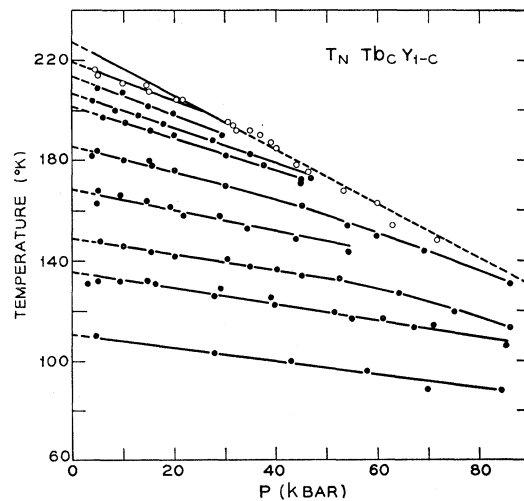


FIG. 5. Effect of pressure on the Néel temperature of the Tb-Y alloys. The top curve is for pure Tb and is given by $T_N = 227 - 1.08P$. The open circles are points for $\text{Tb}_{0.95}\text{Y}_{0.05}$ showing the envelope effect. From top to bottom the curves are for alloys with the following Tb concentration: 1.00, 0.95, 0.90, 0.85, 0.80, 0.70, 0.60, 0.50, 0.40, and 0.30.

temperature decreases more slowly with pressure for $Tb_{0.95}Y_{0.05}$ than for Tb . Instead of the two curves crossing at ~ 25 kbar, they appear to coalesce. Similar effects were observed for the alloys containing 90, 85, and 80% Tb , but the points near and above the intersection of the curves were not included for the sake of clarity in the figure. The initial slopes and Néel temperatures at 1 atm. were obtained from straight lines drawn through the data in the linear regions.

In Fig. 6, the data from the high-pressure phase are plotted. The lines are calculated from the data given in Table I for Tb and Dy . The data for the Tb - Y alloys fall fairly well between the calculated curves for the elements Tb and Dy in agreement with their average De Gennes functions being between those of Tb and Dy . The alloys from pure Tb to $Tb_{0.675}Y_{0.325}$ all order over a fairly narrow temperature range at these pressures considering that the range in the concentration of the nonmagnetic component is 30%. The difference between T_N and $T_N(2a)$ and the pressure at which it was determined is listed in Table I along with the average $(T_{N2a} - T_{N2b})$ for each alloy.

In Fig. 7 the effect of pressure on the Curie temperature of the Tb - Y alloys determined from the warming curves is shown. In view of the problems of hysteresis, etc. shown in Fig. 2, any interpretation of the T_c versus P curves should be made with caution. The hystereses observed in the inflection points increases with increasing Y concentration with $\Delta T_c = 9, 11,$ and $15^\circ K$ for the alloys with 5, 10 and 15% Y , respectively. The initial slopes and intercepts calculated from the smooth curves are $-0.9^\circ K/kbar(204^\circ K)$; $-0.8(180)$; $-1.6(160)$; $-0.2(128)$ for the alloys with 5, 10, 15, and 20% yttrium, respectively. There is a qualitative change in the shape of the curves with concentration. This is complicated by the fact that at the higher pressures in $Tb_{0.85}Y_{0.15}$ and at all pressures in $Tb_{0.8}Y_{0.2}$ the maximum in χ_i was not reached⁹ at $77^\circ K$ on cooling, and on warming χ_i rose to a maximum and then dropped. This condition was simulated in $Tb_{0.95}Y_{0.05}$ and found

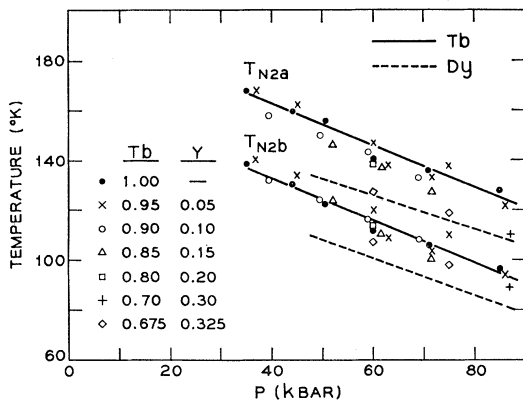


FIG. 6. Effect of pressure on the two peaks of the high-pressure phases in the Tb - Y system. The lines are calculated from the data for pure Tb and Dy .

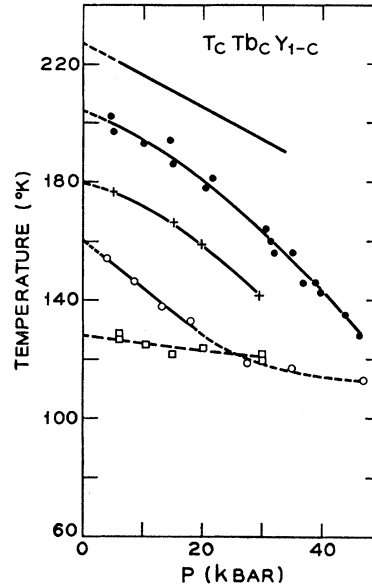


FIG. 7. Effect of pressure on the Curie temperature of the Tb - Y alloys. The top curve is for pure Tb and is the same as the one given in Fig. 5. From top to bottom the curves are for alloys with Tb concentration of 1.00, 0.95, 0.90, 0.85, and 0.80.

to have no effect on the observed T_c , and this suggests that the trend shown in Fig. 7 may be real.

DISCUSSION

The magnetic ordering observed in the rare-earth metals and alloys is believed to be caused by an indirect exchange mechanism via the conduction electrons. It has been shown that in the heavy rare-earth metals this mechanism stabilizes an antiferromagnetic, screw-like structure and that the inclusion of the anisotropy energy can account for the variations in magnetic structure that are observed with increasing atomic number. In a molecular field approximation the Néel temperature for a helical structure is given by the following equations^{9,10}:

$$kT_N = \frac{2}{3}(g-1)^2 J(J+1)J(Q) + \frac{2}{5}K_2(J-\frac{1}{2})(J+\frac{3}{2}) \quad (1)$$

where

$$J(Q) = \sum_{ij} J(\mathbf{R}_{ij}) \exp[i\mathbf{Q} \cdot \mathbf{R}_{ij}], \quad (2)$$

$$J(\mathbf{R}_{ij}) = \sum_{\mathbf{q}} |I(\mathbf{q})|^2 \chi(\mathbf{q}) \exp[i\mathbf{q} \cdot \mathbf{R}_{ij}].$$

As \mathbf{J} is a good quantum number, $\mathbf{S} \rightarrow (g-1)\mathbf{J}$ where g is the Landé factor. \mathbf{Q} is the vector which characterizes the antiferromagnetic screw structure; $\mathbf{R}_{ij} = \mathbf{R}_j - \mathbf{R}_i$ is an interatomic vector; and \mathbf{q} is the scattering vector for a conduction electron from state \mathbf{k} to \mathbf{k}' . The effective exchange interaction $J(\mathbf{R}_{ij})$ involves the product of the conduction electron susceptibility $\chi(\mathbf{q})$ and a form

⁹ R. J. Elliott, in *Magnetism*, edited by G. T. Rado and Harry Suhl (Academic Press Inc., New York, 1965), Vol. IIA.

¹⁰ K. Yosida, in *Progress in Low Temperature Physics*, edited by C. J. Gorter (North-Holland Publishing Company, Amsterdam, 1964), Vol. 4.

factor $I(\mathbf{q})$ which is an exchange integral between the $6s$, $5d$ electrons and the $4f$ electrons. The anisotropy energy is assumed to be represented by the second-order spherical harmonic and is assumed to be much less than the exchange energy.

The $4f$ electrons are well localized so that the change in the magnitude of the magnetic moment at 0°K (σ_0) with volume should be fairly small and the change in the ordering temperature with pressure gives the change in $J(\mathbf{Q})$ directly. The change in σ_0 with pressure can be calculated from measurements of the forced magnetostriction in rare-earth single crystals by the thermodynamic relation

$$[\partial(\Delta V/V)/\partial H]_P = -(\partial\sigma/\partial P)_H.$$

From Rhyne and Legvold's data on Tb^{11} and Monfort and Swenson's¹² compressibility results, one estimates $(d \ln \sigma_0 / d \ln V) \approx 0 \pm 0.2$. The change in the magnetization with pressure has been measured directly at 77°K by Bloch¹³ on polycrystalline material, and his extrapolated results (using Bridgman's compressibilities¹⁴ for Gd and Dy) are

$$\frac{d \ln \sigma_0}{d \ln V} = 0.2(\text{Gd}), 1.4(\text{Tb}), \text{ and } 0.04(\text{Dy}).$$

(The forced magnetostriction measurements on Tb are more reliable as single-crystal material was used.) As the changes in the ordering temperatures with volume $(d \ln T / d \ln V)$ vary from 2.1 (Gd) to 0.8 ($\text{Tb}_{0.3}\text{Y}_{0.7}$), the change in the magnetic moment at 0°K with volume can be neglected and $(g-1)^2 J(J+1)$ can be taken as constant.

The anisotropy energy for the helical structure can be approximated by $-\frac{1}{3}k(\theta_{11}-\theta_{\perp})$ where k is Boltzmann's constant and θ_{11} and θ_{\perp} are the paramagnetic Curie temperatures parallel and perpendicular to the hexagonal axis. This approximation is reasonable for Tb through Ho where the anisotropy energy is $\approx 10\%$ of the total magnetic energy (kT_N). It is also assumed that the anisotropy energy varies as V^{-1} .

Assuming that the magnetic moment at 0°K is independent of pressure and that the anisotropy energy can be approximated by $-\frac{1}{3}k(\theta_{11}-\theta_{\perp})(V_0/V)$, then a value for the exchange integral $J(\mathbf{Q})$ (at the value of \mathbf{Q} which makes $J(\mathbf{Q})$ a maximum) can be calculated from

$$J(\mathbf{Q})/k = \frac{3}{2}X^{-1}[T_N(V) + \frac{1}{3}(\theta_{11}-\theta_{\perp})(V_0/V)], \quad (3)$$

where $X = \sum_i c_i (g_i - 1)^2 J_i (J_i + 1)$ and c_i is the atomic percent of the i th component. Values of $J(\mathbf{Q})$ calculated in this way are plotted in Fig. 8 versus a dimensionless parameter Kr_{4f} where $K = V^{-1/3}$ and r_{4f} is taken from the work of Freeman and Watson ($r_{4f} = \langle r_{4f}^2 \rangle^{1/2}$).¹⁵ The values of K are calculated using the compressibilities of Refs. 12 and 14, and it is assumed that the compressibilities of the alloys vary linearly between those of the end members. r_{4f} is assumed to be independent of volume and is a scaling constant which at least partially accounts for the dependence of $J(\mathbf{Q})$ on the $4f$ electron configuration. Widely varying values for r_{4f} are obtained depending on the method of calculation, and therefore the values used are only indicative of the trend in r_{4f} with atomic number.

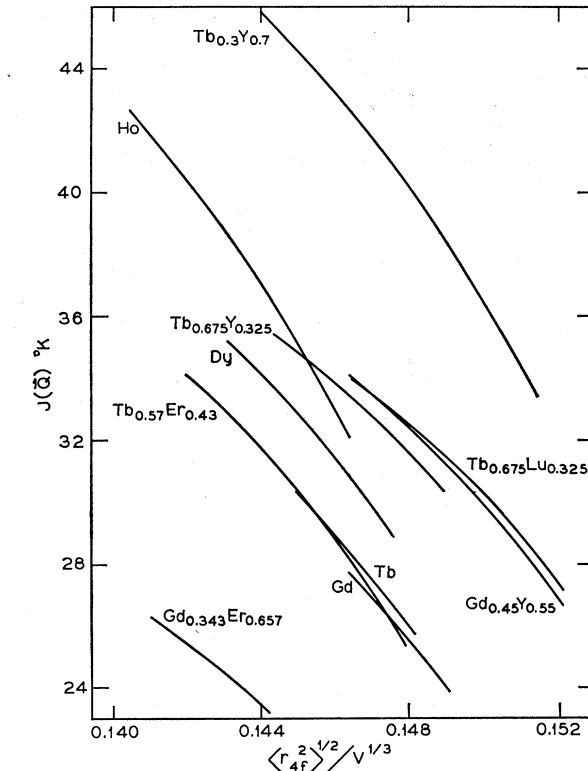


Fig. 8. The variation of the exchange interaction with $\langle r_{4f}^2 \rangle^{1/2} / V^{1/3}$ for several rare-earth elements and alloys. The average slope for all the alloys is $k^{-1}dJ(\mathbf{Q})/d(Kr_{4f}) = -1300 \pm 200^\circ\text{K}$.

The slopes of the curves in Fig. 8 are quite similar for a wide variety of materials, and the average slope is $k^{-1}dJ(\mathbf{Q})/d(Kr_{4f}) = -1300 \pm 200^\circ\text{K}$. Evaluating the derivative at Tb and taking $c/a = 1.58$, the change in the exchange integral with lattice parameter (a) is $k^{-1}dJ(\mathbf{Q})/da = (42 \pm 6)^\circ\text{K}/\text{\AA}$. Because of the small range of Kr_{4f} that is covered and the small variation in c/a in the heavy rare-earth metals, the initial slopes for all the systems studied are approximately the same $[(42 \pm 6)^\circ\text{K}/\text{\AA}]$. Thus the observed variation in dT_N/dP results mainly from the variation in X . As

As the slopes of the curves in Fig. 8 are quite similar for a wide variety of materials, and the average slope is $k^{-1}dJ(\mathbf{Q})/d(Kr_{4f}) = -1300 \pm 200^\circ\text{K}$. Evaluating the derivative at Tb and taking $c/a = 1.58$, the change in the exchange integral with lattice parameter (a) is $k^{-1}dJ(\mathbf{Q})/da = (42 \pm 6)^\circ\text{K}/\text{\AA}$. Because of the small range of Kr_{4f} that is covered and the small variation in c/a in the heavy rare-earth metals, the initial slopes for all the systems studied are approximately the same $[(42 \pm 6)^\circ\text{K}/\text{\AA}]$. Thus the observed variation in dT_N/dP results mainly from the variation in X . As

¹¹ J. J. Rhyne and S. Legvold, Phys. Rev. **138**, A507 (1965).

¹² C. E. Monfort, III and C. A. Swenson, J. Phys. Chem. Solids **26**, 623 (1965).

¹³ D. Bloch, Ann. Phys. (N. Y.) **14**, 193 (1966).

¹⁴ P. W. Bridgman, *Collected Experimental Papers* (Harvard University Press, Cambridge, 1964).

¹⁵ A. J. Freeman and R. E. Watson, Phys. Rev. **127**, 2058 (1962).

dT_N/dP scales with X and not $X^{2/3}$, this suggests that the $\frac{2}{3}$ law⁶ is not a universal one.

$J(\mathbf{Q})$, as shown in Fig. 8, decreases for each of the following changes: (1) decreasing volume, (2) decreasing atomic number (Ho \rightarrow Gd), and (3) decreasing Y concentration (Tb-Y alloys). These effects are related to variations in $\chi(\mathbf{q})$ and $I(\mathbf{q})$ [Eq. (2)]. For example $I(\mathbf{q})$ is not independent of \mathbf{q} but will become negligible for $qr_{4f} > 1$, thus essentially cutting off the summation in Eq. (2).¹⁰ $J(\mathbf{Q})$ will then depend to some extent on qr_{4f} which is related to Kr_{4f} . Recent treatments of anisotropic exchange have used an expansion parameter $k_f r_{4f}$ where k_f is the Fermi wave vector.^{16,17} However, the changes in $J(\mathbf{Q})$ with volume, atomic number, and dilution are probably principally related to changes in $\chi(\mathbf{q})$, and the theory has not yet been developed to the point where the appropriate variations in the band structure can be calculated with the necessary precision. The recent band-structure calculations for the rare-earth metals show that the band structures are more similar to those of the transition metals than to the free-electron model.¹⁸⁻²¹ However, the free-electron model can be used to show that the observed pressure dependence of $J(\mathbf{Q})$ probably results from changes in the density of states at the Fermi surface.

Liu²² has shown that in a free-electron approximation for the conduction electrons,

$$\frac{d \ln T_c}{d \ln V} = \frac{\partial \ln N(E_F)}{\partial \ln V} + \frac{2 \partial \ln I}{\partial \ln V}, \quad (4)$$

where $N(E_F)$ is the density of states per atom at the Fermi energy and I is the s - f exchange integral. If anisotropy effects are neglected, Eq. (6) also holds for the paramagnetic to antiferromagnetic transition (T_N). The experimental values for the rare-earth metals and the Tb-Y alloys are plotted in Fig. 9. The data for the elements were discussed in Ref. 1, and the points for Ce and Nd were calculated by Andres²³ from low-temperature thermal expansion measurements. The value of $[\partial \ln N(E_F)/\partial \ln V]$ in Eq. (4) can be approximated by the electronic Grüneisen parameter.²³ As the conduction bands in the heavy rare-earth metals are transition metal-like, the order of magnitude of $[\partial \ln N(E_F)/\partial \ln V]$ may be comparable to γ_e for Pt(2.5) or Ta(1.2) [Pt and Ta have values of $N(E_F)$ comparable to that calculated for Gd].¹⁸ This suggests that most of the observed variation in T_N with volume can

¹⁶ T. A. Kaplan and D. H. Lyons, Phys. Rev. **129**, 2072 (1963).

¹⁷ T. Kasuya and D. H. Lyons, J. Phys. Soc. (Japan) **21**, 287 (1966).

¹⁸ J. O. Dimmock and A. J. Freeman, Phys. Rev. Letters **13**, 750 (1964).

¹⁹ A. J. Freeman, J. O. Dimmock, and R. E. Watson, Phys. Rev. Letters **16**, 94 (1966).

²⁰ R. W. Williams, T. L. Loucks, and A. R. Mackintosh, Phys. Rev. Letters **16**, 168 (1966).

²¹ T. L. Loucks, Phys. Rev. **144**, 504 (1966).

²² S. H. Liu, Phys. Rev. **127**, 1889 (1962).

²³ K. Andres, Phys. Kondensierten Materie **2**, 294 (1964).

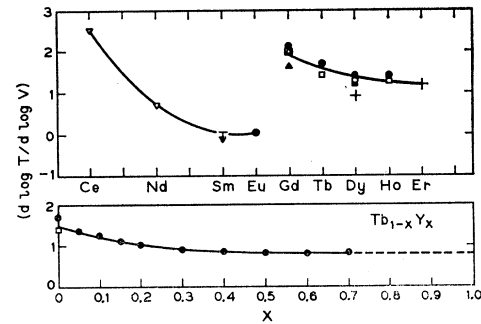


Fig. 9. Variation of $d \ln T / d \ln V$ with atomic number and concentration. ∇ Ref. 23; \circ Ref. 2; \square Ref. 13; \blacktriangle L. Patrick, Phys. Rev. **93**, 384 (1954); \triangle L. B. Robinson, F. Milstein, and A. Jayaraman, *ibid.* **134**, A187 (1964); \circ P. C. Souers and G. Jura, Science **145**, 575 (1964); \blacksquare P. Landry and R. Stevenson, Can. J. Phys. **41**, 1273 (1963); $+$ J. E. Milton and T. A. Scott, Bull. Am. Phys. Soc. **11**, 527 (1966).

be attributed to the variation of the density of states with volume.

For a more realistic band structure of the rare-earth metals, the \mathbf{q} dependence of $\chi(\mathbf{q})$ will be quite complex. However, $\chi(0)$ can be estimated from the electronic specific heat, if electron-phonon interactions are neglected, and from x-ray isochromats. Both measurements show that $\chi(0)$ is approximately constant across the heavy rare-earth metals.^{24,25} This suggests that the change in $J(\mathbf{Q})$ with atomic number results from changes in the \mathbf{q} dependence of $\chi(\mathbf{q})$. As $dJ(\mathbf{Q})/da$ is similar for the range of materials shown in Fig. 8, this suggests that the volume dependence of $\chi(\mathbf{q})$ is also similar for the different materials even though the \mathbf{q} dependence varies.

Turning to the magnetic properties of the high-pressure phase, a striking similarity is observed in a wide variety of materials. The difference in the ordering temperatures of the hcp and Sm-type phases ($T_{N1} - T_{N2a}$, Table I) is about 10% for all the samples. Presumably the difference in ordering temperature results mainly from the variation in the band structure with changes in symmetry.

Of equal interest are the two ordering temperatures observed in the Sm-type phase itself. The percent difference, $(T_{N2a} - T_{N2b})/T_{N2a}$, is $\approx 17\%$ for the different samples. One possible explanation for the two ordering temperatures is that by analogy with Nd the two different crystallographic sites order independently at different temperatures.²⁶ Another possibility is that the lower ordering temperature represents a transition from one type of ordered structure to another as, for example, is found in Er.⁷ The curve of χ_i versus T for $\text{Tb}_{0.54}\text{Er}_{0.43}$ in Fig. 4, which is an example of T_N followed by an order-order transition, is different from

²⁴ O. V. Lounasmaa, Phys. Rev. **133**, A219 (1964).

²⁵ Staffan Bergwall, Z. Physik **193**, 13 (1966).

²⁶ R. M. Moon, J. W. Cable, and W. C. Koehler, J. Appl. Phys. **35**, 1041 (1964).

curves of χ_i versus T observed in the different Sm-type phases. The peaks are much more symmetrical in the latter cases. The biggest problem with both explanations is to find the cause of the two transitions. The order-order transitions in the heavy rare earths have been explained on the basis of the interaction of the 4f electrons with the crystal field.^{9,10} However, in Gd the 4f electrons are in an S state and the crystal-field effects must be two orders of magnitude lower than in Tb, Dy, and Ho. However, the percent difference between the two ordering temperatures is about the same for all the materials studied. This suggests that the origin is not the 4f electrons but the conduction electrons.

The present study shows that a hcp-Sm-type transition is found in a wide variety of heavy rare-earth alloys. The trend in structure in the rare-earth metals with increasing pressure is the same as that found with decreasing atomic number. This trend was proposed by Jayaraman on the basis of the transitions in Gd⁴ and Sm.⁵ Jayaraman *et al.*,²⁷ have recently shown that this trend is also observed with increasing pressure in some alloys of the lighter rare earths with Y and with the heavy rare earths. In Ref. 1 x-ray diffraction data obtained at high pressure was presented which suggested that Tb, Dy, and Ho by analogy with Gd have a hcp \rightarrow Sm-type transition. Recently, Perez-Albuerne *et al.* found transitions in Ho, Er, and Tm by x-ray methods.²⁸ Thus in all the heavy rare-earth metals with the exception of Lu, transitions have been observed with increasing pressure. The transition pressures at room temperature increase smoothly with increasing atomic number: 25 kbar (Gd), 30 (Tb), 45 (Dy), 65 (Ho), 90 (Er), and 110 (Tm). The present study indicates a similar increase in transition pressure with increasing Y concentration in the Tb-Y alloys. It was noted that in the series of alloys having equal average De Gennes functions the transition was observed in the magnetic measurements at different pressures. X-ray diffraction studies at high pressures confirm that the break in the plot of the diffraction angles $\theta_{10,0}$ versus $\theta_{10,1}$ (Ref. 1), which indicates the onset of the transi-

tion, is in the volume sequence Dy, Tb_{0.675}Y_{0.325} > Tb_{0.57}Er_{0.43} > Tb_{0.675}Lu_{0.325}.²⁹ A transition was not observed within our pressure range ($P < 85$ kbar) for Gd_{0.45}Y_{0.55}. Originally it was thought that the occurrence of the hcp \rightarrow Sm-type transition was related to an increase in the c/a ratio with pressure toward the ideal value. Early x-ray studies seemed to support this conclusion. However the effect of pressure on the c/a ratio of Gd was recently studied using a high-pressure guinier-type focusing camera and *no* change in c/a was observed up to 25 kbar [$(V_0 a_0/c_0)(\Delta(c/a)/\Delta V) = 0 \pm 0.06$].²⁹ A re-examination of the earlier data showed that using only the d spacings for the 10.0 and 10.1 reflections leads to erroneous results. Because the a parameter depends on $\theta_{10,0}$, it is subject to absorption and eccentricity errors. The c parameter essentially depends on the difference $\sin^2\theta_{10,1} - \sin^2\theta_{10,0}$, and the errors are greatly reduced because both $\theta_{10,0}$ and $\theta_{10,1}$ are in the same angular range. By using all six observable reflections to determine the parameters, this problem is minimized. A re-examination of the older data on Gd, Tb, Dy and Ho in this way suggests that the change in c/a with pressure is in fact very small and that the onset of the transition cannot be correlated in this way.

The occurrence of this trend in structure reflects small differences in the energy of the conduction electron system resulting from the changes in symmetry. Probably both the structural trend and the two ordering temperatures in the Sm-type phase reflect this change. Also, this would be consistent with trying to account for the observed variation in $J(\mathbf{Q})$ in the hcp phase on the basis of changes in the shape of the Fermi surface. It would be interesting to see if band structures calculated by the augmented plane wave method do show reasonable changes with structure. However, definitive information on these different effects will have to be obtained by neutron scattering studies at high pressure.

ACKNOWLEDGMENTS

The authors thank K. Andres, A. C. Gossard, C. Herring, and A. Jayaraman for helpful discussions and E. Corenzwit for making the samples.

²⁷ A. Jayaraman, R. C. Sherwood, H. J. Williams, and E. Corenzwit, Phys. Rev. **148**, 502 (1966).

²⁸ E. A. Perez-Albuerne, R. L. Clendenen, R. W. Lynch, and H. G. Drickamer, Phys. Rev. **142**, 392 (1966).

²⁹ D. B. McWhan (unpublished).